Available online at www.sciencedirect.com
ScienceDirect
Microvascular Research 75 (2008) 211–216
Microvascular Research
www.elsevier.com/locate/ymvre

Regular Article

Effects of angiotensin II on flux rise time in rats (a time index of laser Doppler flowmetry) and its relation with microvascular structures

Tse Lin Hsu [a,b], Pin Tsun Chao [b], Ming Yie Jan [b], Wei Kung Wang [b], Sai Ping Li [b], Yuh Ying Lin Wang [a,b,*]

[a] *Department of Physics, National Taiwan Normal University, Taipei, ROC, Taiwan*
[b] *Biophysics Lab, Institute of Physics, Academia Sinica, Nankang, Taipei, ROC 11529, Taiwan*

Received 12 January 2007; revised 15 May 2007; accepted 13 July 2007
Available online 3 August 2007

Abstract

Laser Doppler flowmetry (LDF) is a popular method for monitoring the microcirculation, but it does not provide absolute measurements on local area with small size microvessels. Instead, the mean flux response is generally compared between before and after stimulus. In this study, we proposed a new dimension for comparing the LDF signals. The flux rise time (FRT), a time index with absolute physical quantity, was extracted from noisy LDF signals using a pulsatile-based synchronized-averaging method. We investigated the changes of FRT and its relation to the microvascular resistance (MVR) under the selective effects of angiotensin II (Ang II) on the kidney and the plantar palm. Ang II was infused into anesthetized Wistar Kyoto rats via the femoral vein for 1 h. Using the heartbeat as a self-trigger, we calculated the FRT and MVR from the renal cortical flux, plantar palm flux, and abdominal aortic blood pressure recorded before, during, and after Ang II infusion. The control FRT values were similar in the two vascular beds. Ang II decreased the renal cortical flux but significantly increased the FRT and MVR of both beds. The effects on the renal FRT and renal MVR were selectively larger than those on the palm FRT and palm MVR. The results indicate that the changes of FRT and MVR are similarly physiologically linked with microvascular structures. As an MVR-related absolute physical quantity, the FRT could be developed as a monitoring tool in physiological, pathological, and pharmacological investigations.

Keywords: Microvascular resistance; Vasoconstriction; Laser Doppler flowmetry; Angiotensin II; Flux rise time

Introduction

Laser Doppler flowmetry (LDF) is a popular method for monitoring microcirculation. It has clinical advantages such as being noninvasive and able to measure rapid responses, but it also has the drawbacks of yielding data that are noisy and reflect only relative averaging values on local area with small size microvessels (arterioles and capillaries) (Shepherd, 1990). Since LDF on local area is commonly used for comparative studies of the long-term DC flux response to external stimulation, the pulsatile (i.e., AC) component of the LDF signal is usually filtered out as noise, whereas either the pulsatility indexes from LDF studies on the large individual major vessel (Grunwald et al., 1988; Petrig and Riva, 1991) or the pressure pulse studies (Hsu et al., 2005) all indicate that AC component may elucidate specific characteristics of the physiological system. To solve these problems, we have previously developed a pulsatile-based signal processing method for LDF signals on local area with small size microvessels (Chao et al., 2006). Since the blood pressure and the peripheral perfusion are coherent with a phase difference that varies only slightly between individuals (Jan et al., 2000; Seki et al., 2004), treating the blood pressure as the stimulus and the recorded LDF data as the evoked signal allows a time-domain synchronized-averaging method (Rangrraj, 2002) to be used in separating the pulsatile component of the LDF signals from the noise (Jan et al., 2000). A similar technique has been used in pulsatility index study for extracting the pulsatile component of the LDF signal on large individual major vessel (Grunwald et al., 1988; Petrig and Riva, 1991). From the extracted pulsatile component

* Corresponding author. Department of Physics, National Taiwan Normal University, Taipei, Taiwan. Fax: +886 2 27880058x2050.
E-mail address: yuhying@phy.ntnu.edu.tw (Y.Y.L. Wang).

0026-2862/$ - see front matter © 2007 Elsevier Inc. All rights reserved.
doi:10.1016/j.mvr.2007.07.006

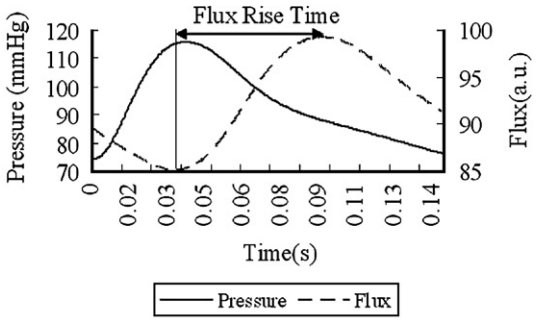

Fig. 1. Typical averaged pressure pulse (solid line) and flux pulse (dashed line) profiles, indicating the time index FRT. *a.u.: arbitrary units.

of the local area LDF signals, the flux rise time (FRT) can be used as a time index, which is the time taken for the flux to go from the lowest point to the highest point in a cardiac cycle (Fig. 1), and which may be linked to the physiological properties of the flux driving mechanism as well as the underlying anatomy (Chao et al., 2006).

Frank and Hochmuth (1988) reported that the rise time (as a delayed peak) of the resistive pulse for a single red blood cell flowing through individual capillary-sized pores will be lengthened due to cell deformation by an amount dependent on both the pore size and cell deformability. This may be the origin of FRT, which represents the collective behavior of multiple red blood cells in a small area of microvessels (including capillaries and arterioles) under the fixed LDF scattering volume.

A longer FRT corresponds to a delayed peak in the flux, which may be attributable to the collective behavior of the delayed peak (lengthening of rising time) of resistive pulse due to a longer-than-average time for erythrocytes to enter into microvessels (Frank and Hochmuth, 1988). Under a similar driving force, a longer entrance time might be due to smaller-diameter microvessels (Frank and Hochmuth, 1987, 1988; Secomb and Hsu, 1996; Jan et al., 2000; Drochon, 2005; Chao et al., 2006) exhibiting a higher microvascular resistance (MVR). The FRT and MVR might be similarly physiologically linked with microvascular structures. As an evidence of our notions, we previously (Chao et al., 2006) showed that the renal FRT (R_FRT) as measured from renal cortical flux signals was significantly longer in spontaneous hypertensive rats than in Wistar Kyoto (WKY) rats, which coincides with differences between the renal microvascular structures of these rat types. Another support is that the FRT calculated from the LDF signal on large artery (such as the renal artery) is much smaller (data not published) than the FRT calculated from the LDF signal on local area with small microvessels.

To explicit the linkage between the FRT time index and microvascular structures, a study on the relations between the changes of FRT and MVR was conducted in this report. We investigated the selective effects of angiotensin II (Ang II) on the FRT and MVR in rat renal cortical and plantar palm vascular beds, which exhibit differing microvascular structures and Ang II responses.

Yamamoto et al. (2001a,b) found that WKY renal arterioles are of small diameter: 11.9±0.2 and 8.9±0.2 μm for afferent and efferent arterioles, respectively. Ang II causes potent constriction in both afferent and efferent arterioles in the superficial renal cortex (Arendshorst et al., 1999; Denton et al., 2000; Yamamoto et al., 2001a,b).

On the other hand, according to Rendell et al. (1998), the plantar palm exhibits a high density of capillaries and a high degree of arteriovenous (A–V) shunting that contains a higher proportion of much larger diameter arterioles (21.6±1.0 μm) compared to capillaries in WKY rats. Nonetheless, most of these larger diameter arterioles that are used for heat regulation are at rest in the baseline condition. During Ang II infusion blood flow may be redirected from large functional arterioles to small nutritive capillaries in the plantar palm, as reported for the rat hind limb (Zhang et al., 2005).

All the above complicate events on microvessels may affect the FRT and MVR. It was expected that we may resolve the relations between the FRT, MVR, and these events. The advantages of using LDF to measure the FRT time index as an absolute physical quantity (comparing to the relative MVR value) may lead to its development as a powerful clinical tool. Under well-controlled conditions, a carefully investigated absolute FRT baseline value with known intra- and inter-person changes may provide a person's basal health condition directly without extra-stimulation test.

Materials and methods

Animal preparation and experimental setup

The investigation conformed to the "Guide for the Care and Use of Laboratory Animals" published by the U.S. National Institutes of Health. Nine male WKY rats weighing 240–320 g were obtained from the Experimental Animal Center of National Taiwan University, Taipei, Taiwan. The animals were housed in our animal care facility with a 12-h light/12-h dark cycle for at least 1 week before experiments were conducted. They received water and food *ad libitum* (Labdiet 5001 rodent diet, PMI Nutrition International, Brentwood, MO, USA) prior to the experiments.

Fig. 2 illustrates the experimental setup. The rats were anesthetized with urethane only (1.1 g kg^{-1} 2 ml^{-1} in saline, i.p.) (Sigma, St. Louis, MO, USA). A heating pad was used to maintain the body temperature.

The femoral vein was exposed through an inguinal incision, and drug infusion was provided via a polyethylene cannula (PE-10, i.d. 0.28 mm, o.d. 0.61 mm) by a pump at a rate of 5 μl min^{-1} (Gilson Minipuls 2, Gilson Medical Electronics, Middleton, WI, USA).

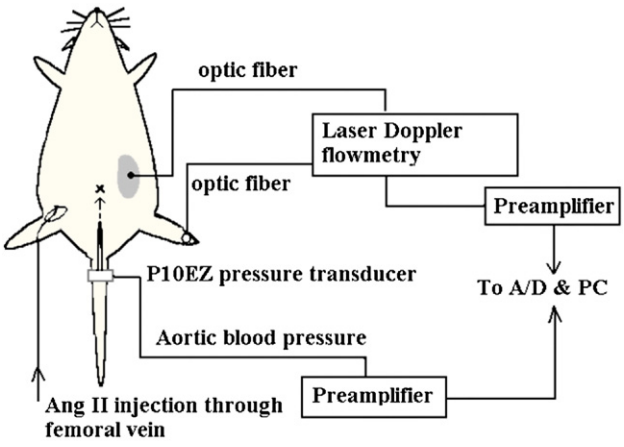

Fig. 2. Experimental setup.

The tail artery was cannulated with an intravenous catheter (Angiocath Plus, 22 gauge needle size, 1.00 in. needle length, 0.9×25 mm^2, Becton-Dickinson, Seoul, Korea) filled with physiological saline and heparin (1.5 g kg^{-1} 2 ml^{-1} in saline), which was connected to a pressure transducer (P10EZ Ohmeda, Singapore). The cannulation opening in the tail artery was about 1 cm from the anus. The abdominal aortic blood pressure (AABP) pulse was then passed through the catheter tip to the pressure transducer.

A small area (~0.5×0.5 cm^2) of the left kidney was exposed from the dorsal side. The fatty capsule was carefully pushed aside using sterilized gauze sponges, and the surface of the kidney was infused with normal saline at 37 °C to keep it moist during the experiments. An LDF optical fiber probe (P10M+P17, Moor Instruments, Devon, UK) was held perpendicular against the surface of the renal cortex to acquire the renal cortical flux signal with a time constant of 0.02 s and a cut-off frequency of 14.9 kHz.

The left plantar palm of the experimental animal was cleaned gently with warm water, and then the LDF probe (P10, Moor Instruments) was fixed at the center of the palm with Scotch tape to acquire the plantar palm flux signal.

Data acquisition

A flowchart for data acquisition is given in Fig. 3. The abdominal aortic blood pressure and LDF signals were sampled synchronously with a sample-and-hold card (AX753, Axiom Technology, Hsin Tien, Taiwan) and sent to an A/D converter card (AX5621, Axiom Technology) at a sampling rate of 3000 Hz.

After all the operations were completed, saline was infused continuously into the femoral vein at a rate of 5 μl min^{-1} to prevent dehydration, and at least another 180 min was allowed for stabilization. A 10-s pulse sequence (comprising 50–80 pulses) was then acquired every minute, with 20 data sequences being recorded over a 20-min period as baseline data.

To ensure that the experimental animal was in a normal and stable physiological condition, we required that the coefficient of variance (CV=SD/mean) for the baseline heart rate and diastolic pressure to be less than 3%, and the mean blood pressure to be in the range 85–110 mm Hg. If the CV or the mean blood pressure did not satisfy its criterion, the animal was considered unstable and the data were discarded.

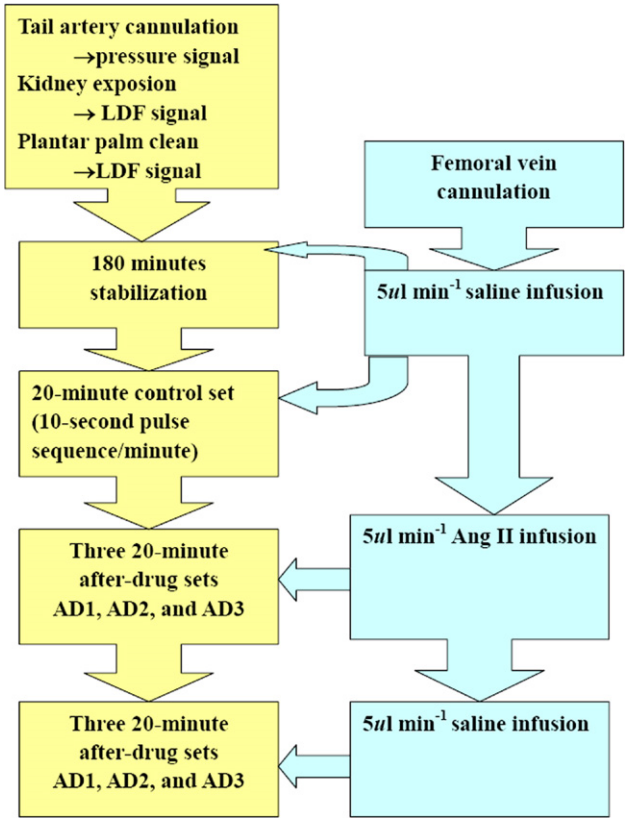

Fig. 3. Flowchart for data acquisition.

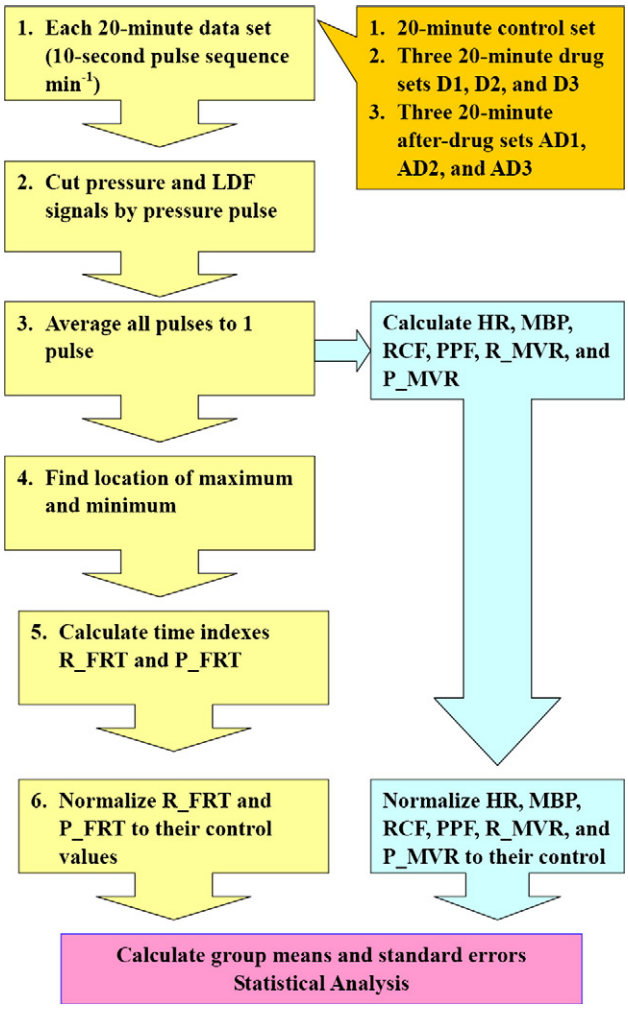

Fig. 4. Flowchart for signal processing.

After the control period, the saline infusion was replaced with Ang II at the same rate for 1 h. Ang II was dissolved in saline at a concentration of 20 pmol 5 μl^{-1}. We recorded 60 data sequences over 60 min as drug data, and then the following 60 data sequences as after-drug data during which saline was again infused. The data sequences were divided into three 20-min drug sets (D1, D2, and D3) and three 20-min after-drug sets (AD1, AD2, and AD3).

Signal processing of the pulsatile component

A signal processing flowchart is given in Fig. 4. Data sets containing obvious motion artifacts were discarded. Unlike traditional LDF signal processing in which a low-pass filter is used to eliminate the pulsatile component, we used anti-noise time-domain synchronized-averaging (Rangrraj, 2002) to enhance the pulsatile component of the LDF signal (Grunwald et al., 1988; Petrig and Riva, 1991; Jan et al., 2000). Here we treated the blood pressure wave as the stimulus signal and the LDF signal as the evoked signal.

Each 20-min data set contained 1000–1600 pulses, depending on the HR of the individual rate. We utilized the quasiperiodic nature and explicit diastolic turning points of the blood pressure waveform to separate each pulse by identifying the cardiac component according to the two neighboring lowest points. The flux wave was then cut at the same cut point, and the cut segments were synchronously averaged into one averaged segment. The heart rate, the mean blood pressure, the renal cortical flux, the plantar palm flux, and the time indexes R_FRT and P_FRT were calculated in these averaged segments, and the

Table 1
Basic physiological parameters (mean±SE, $n=9$)

Body weight (g)	Heart rate (beats s^{-1})	Blood pressure (mm Hg)	
293.53±25.18	6.80±0.15	93.46±2.77	
R_FRT (ms)	P_FRT (ms)	Renal cortical flux (a.u.)[a]	Plantar palm flux (a.u.)[a]
60.59±0.92	60.64±1.47	101.6±4.4	95.4±5.8

[a] a.u.: arbitrary units.

ratio of the mean blood pressure to the renal cortical flux or the plantar palm flux was computed as the index of R_MVR or P_MVR, respectively.

Statistical analyses

Since only the relative values of the renal cortical flux, the plantar palm flux, R_MVR, and P_MVR are meaningful, we normalized all these variables to the control values for each animal before performing further group averaging and statistical comparisons. The absolute values of the group means and standard errors (SEs) of the heart rate, the mean blood pressure, R_FRT, and P_FRT were calculated for the control stage only.

Student's paired *t*-test was used for statistical comparisons. The drug effects were considered to be significantly different from the control if $p<0.05$.

Results

Table 1 lists the group means and SEs of the control body weight, the heart rate, the mean blood pressure, the renal cortical flux, the plantar palm flux, R_FRT, and P_FRT. The control values of the P_FRT and R_FRT were similar, but the P_FRT exhibited a larger SE. The relative effects of Ang II on the heart rate, the mean blood pressure, the renal cortical flux, the plantar palm flux, R_FRT, P_FRT, R_MVR, and P_MVR are shown in Fig. 5. Ang II increased the mean blood pressure, R_FRT, P_FRT, R_MVR, and P_MVR but decreased the heart rate and the renal cortical flux significantly. Ang II had no significant effect on the plantar palm flux, and its effect was smaller on the plantar palm than on the kidney.

Discussion

In this study, we measured the selective effects of Ang II on the MVR and the LDF-measured FRT time index in the renal and plantar vascular beds. The control values of the R_FRT and P_FRT were similar, but the P_FRT is less stable. Ang II exerted significant effects on the MVR and FRT in both vascular beds. The effects on the P_FRT and P_MVR were selectively smaller than those on the R_MVR and R_FRT. These results are discussed as follows:

Vascular structure influences on FRT and MVR

As we have mentioned in the introduction, a longer FRT may be attributable to a longer average entrance time for erythrocytes to get into microvessels due to their smaller average diameter, which will result in a higher membrane viscous resistance and in consequence a higher MVR (Secomb and Hsu, 1996; Drochon, 2005). However, because the larger the vessel diameter is, the less cell deformation will be needed; there will be a critical blood vessel diameter, above which cells can enter into without deformation, and hence the entrance time will exhibit a minimum regardless of the vessel diameter. Therefore, the FRT may more precisely be described as the averaged "difficulty" of erythrocytes getting into microvessels of a vascular bed with large arterioles such as an A–V site.

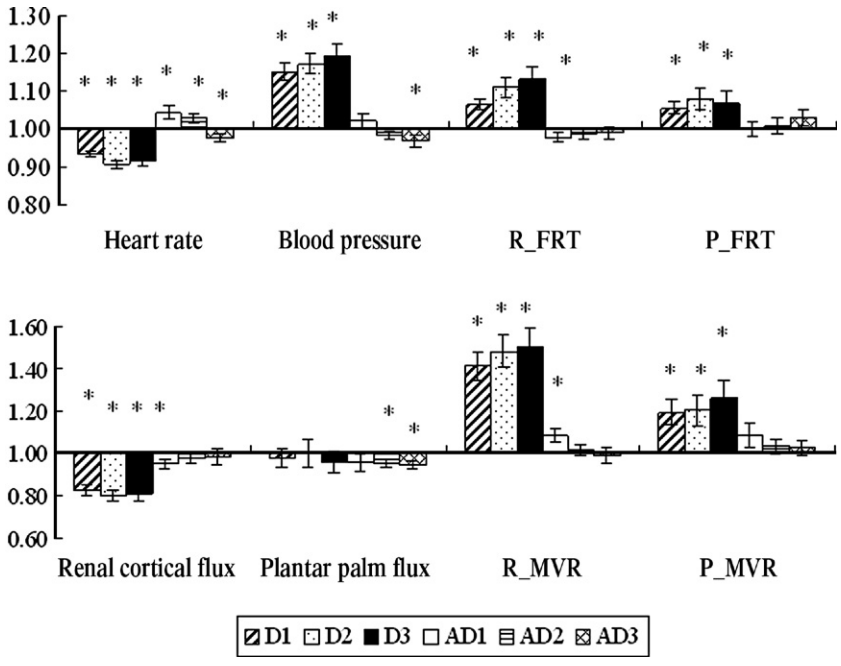

Fig. 5. Relative group mean and SE values of the heart rate, the mean blood pressure, the renal cortical flux, the plantar palm flux, R_FRT, P_FRT, R_MVR, and P_MVR during (D1, D2, and D3) and after (AD1, AD2, and AD3) Ang II infusion. Each time interval was 20 min. *Drug effects differ significantly from control ($p<0.05$).

Control stage

The similar control FRT values observed in the two vascular beds indicate that the two vascular beds exhibit similar averaged "difficulties" for erythrocytes getting into microvessels. Since it is much easier for erythrocytes getting into the large plantar arterioles than the smaller renal arterioles, the ratio of capillaries to arterioles that are participating in the blood flow should be higher in the planter palm than in the kidney so that the similar averaged "difficulties" could be reached. The above inference explains the physiological necessity for the high density of capillaries in the paw (Rendell et al., 1998). The inference is also supported by the evidence that most of the larger diameter arterioles in the plantar palm (used for heat regulation) are at rest in the baseline condition.

A common baseline value of the FRT in different vascular beds with different blood flows indicates that the averaging "difficulties" for erythrocytes to get into the microvessels, the averaging diameter of the flow participating microvessels, the averaging cell entrance time, as well as the averaging cell membrane viscous resistances due to red blood cell deformation are all similar in these vascular beds on basal condition. The hindered physiologic and clinical meaning of this phenomenon is important; it needs to be explored on more different vascular beds in further studies. FRT may provide a useful standard for evaluating the physiological states of local microvessels.

FRT variations during vasoconstriction

Ang II infusion induces potent constriction in both the afferent and efferent arterioles in superficial renal cortex (Arendshorst et al., 1999; Yamamoto et al., 2001a,b). Potent constriction in these small size arterioles will reduce their diameters to red blood cell comparable size and therefore cause big problem for erythrocytes to enter in. The rise time for the flow of erythrocytes may increase significantly once the diameters of the small efferent and afferent arterioles are further reduced and more serious deformation is needed; the significant increase in the R_FRT is a consequence of the constricted efferent and afferent arterioles.

On the other hand, the constriction of the large-diameter arterioles in the plantar palm may have much less influence on the P_FRT changes. These large arterioles can hardly be constricted to a size comparable to red blood cells, and hence the entrance time for the flow of erythrocytes through the constricted large arterioles will not differ greatly from the control state. Instead, the smaller but significant lengthening of the P_FRT may be due to a change in the flow route. During Ang II infusion, blood flow on plantar palm will be redirected from large functional arterioles to small nutritive capillaries, as reported for the rat hind limb (Zhang et al., 2005). Therefore, the ratio of capillaries to arterioles that are participating in the blood flow is increased, the averaging vessel diameter is decreased which may be responsible for the P_FRT increasing.

MVR variations during vasoconstriction

Denton et al. (2000) showed that the presence of larger diameter arterioles could lessen the effects on vascular resistance of Ang-II-mediated diameter changes. The relative MVR variations depend on the percentage change in the vessel diameter rather than on the absolute change. A significant increase in the R_MVR is a consequence of the constricted small efferent and afferent arterioles. The large plantar arterioles are responsible for the smaller relative increase in the P_MVR during vasoconstriction. The membrane viscous resistance (Secomb and Hsu, 1996) or the "difficulty" of erythrocytes getting into microvessels may play an important role in this phenomenon. Ang II exerted similar effects on the FRT and MVR. The changes of FRT and MVR are similarly physiologically linked with the changes of the microvascular structures.

Stability of FRT

The P_FRT is less stable than the R_FRT, as indicated by the SE values in Table 1. We also found that the 5-min intra-animal CV was much larger for the P_FRT than for the R_FRT (data not shown). The timing of on–off switching of the functional plantar arterioles for heat regulation may be responsible for this instability. In this long-term drug–effect study, we chose 20 min as the sampling interval so as to minimize the intra-animal variance between the two vascular beds. However, as we stated previously (Chao et al., 2006), the CV of the R_FRT remained small in the stable renal bed even when the data sampling interval was shortened from 20 min to 1 min. The variance of the FRT will determine the ultimate temporal resolution for drug effects.

Relation between heart rate and FRT

It is evident that FRT lengthening is not a consequence of the pulse lengthening (decrease in the heart rate) during Ang II infusion. The relative variation in the R_FRT is larger than the relative pulse lengthening, and the vessel constriction influences on the FRT differ in different vascular beds.

This study involved a detailed investigation of the LDF-measured time index FRT. Ang II exerted similar effects on the FRT and MVR. As an MVR-related absolute physical quantity, our results suggest that the FRT could be developed into a useful tool for pharmaceutical investigations. A deeper understanding of the FRT in different vascular structures also clears some obstacles for its direct clinical usage, such as for evaluating the fingers (extremities) of diabetics, burned skin, and transplanted skin or organs, as we have discussed previously (Chao et al., 2006). Using the synchronized-averaging method to acquire the new time index, FRT does not require the placement of measurement devices on tiny arterioles, which may maximize the benefits of LDF such as its noninvasiveness and ability to measure rapid responses.

Acknowledgments

This study was supported in part by the National Science Council, Taiwan, under grant no. NSC-95-2112-M-001-010.

References

Arendshorst, W.J., Brannstrom, K., Ruan, X., 1999. Actions of angiotensin II on the renal microvasculature. J. Am. Soc. Nephrol. 10 (Suppl 11), S149–S161.

Chao, P.T., Jan, M.Y., Hsiu, H., Hsu, T.L., Wang, W.K., Wang Lin, Y.Y., 2006. Evaluating microcirculation by pulsatile laser Doppler signal. Phys. Med. Biol. 51, 845–854.

Denton, K.M., Anderson, W.P., Sinniah, R., 2000. Effect of angiotensin II on regional afferent and efferent arteriole dimensions and the glomerular pole. Am. J. Physiol., Regul. Integr. Comp. Physiol. 279, 629–638.

Drochon, A., 2005. Use of cell transit analyzer pulse height to study the deformation of erythrocytes in bicrochannels. Med. Eng. Phys. 27, 157–165.

Frank, R.S., Hochmuth, R.M., 1987. An investigation of particle flow through capillary models with the resistive pulse technique. ASME J. Biomech. Eng. 109, 103–109.

Frank, R.S., Hochmuth, R.M., 1988. The influence of red cell mechanical properties on flow through single capillary-sized pores. ASME J. Biomech. Eng. 110, 155–160.

Grunwald, J.E., Riva, C.E., Kozart, D.M., 1988. Retinal circulation during a spontaneous rise of intraocular pressure. Br. J. Ophthalmol. 72, 754–758.

Hsu, T.L., Hsiu, H., Chao, P.T., Li, S.P., Wang, W.K., Wang Lin, Y.Y., 2005. Three-block electrical model of renal impedance. Physiol. Meas. 26, 287–399.

Jan, M.Y., Hsiu, H., Hsu, T.L., Wang Lin, Y.Y., Wang, W.K., 2000. The importance of the pulsatile microcirculation in relation to hypertension. IEEE Eng. Med. Biol. 19, 106–111.

Petrig, B.L., Riva, C.E., 1991. Near-IR retinal laser Doppler velocimetry and flowmetry: new delivery and detection techniques. Appl. Opt. 30 (16), 2073–2078.

Rangrraj, M.R., 2002. Filtering for removal of artifacts. In: Kartalopoulos, S.V. (Ed.), Biomedical Signal Processing: A Case-Study Approach. John Wiley & Sons Inc., NY, pp. 94–99.

Rendell, M.S., Finnegan, M.F., Healy, J.C., Lind, A., Milliken, B.K., Finney, D.E., Bonner, R.F., 1998. The relationship of laser Doppler skin blood flow measurements to the cutaneous microvascular anatomy. Microvas. Res. 55, 3–13.

Secomb, T.W., Hsu, R., 1996. Analysis of red blood cell motion through cylindrical micropores: effects of cell properties. Biophys. J. 71, 1095–1101.

Seki, J., Satomura, Y., Ooi, Y., 2004. Velocity pulse advances pressure pulse by close to 45 degrees in the rat pial arterioles. Biorheology 41 (1), 45–52.

Shepherd, A.P., 1990. History of laser-Doppler blood flowmetry. In: Shepherd, A.P., Oberg, P.A. (Eds.), Laser-Doppler Blood Flowmetry. Kluwer Academic Publishers, Norwell, Massachusetts, pp. 1–16.

Yamamoto, T., Hayashi, K., Matsuda, H., Kubota, E., Tanaka, H., Ogasawara, Y., Nakamoto, H., Suzuki, H., Saruta, T., Kajiya, F., 2001a. In vivo visualization of angiotensin II- and tubuloglomerular feedback-mediated renal vasoconstriction. Kidney Int. 60, 364–369.

Yamamoto, T., Tomura, Y., Tanaka, H., Kajiya, F., 2001b. In vivo visualization of characteristics of renal microcirculation in hypertensive and diabetic rats. Am. J. Physiol., Renal Fluid Electrolyte Physiol. 281, F571–F577.

Zhang, L., Newman, J.M.B., Richards, S.M., Rattigan, S., Clark, M.G., 2005. Microvascular flow routes in muscle controlled by vasoconstrictors. Microvas. Res. 70, 7–16.